Nanoscale

PAPER

View Article Online
View Journal | View Issue

Cite this: *Nanoscale*, 2025, **17**, 4439

Colorimetric detection of oxidizing metal ions using anilide-poly(phenylacetylene)s†

Manuel Núñez-Martínez, ‡ Manuel Fernández-Míguez, ‡ Emilio Quiñoá and Félix Freire *

Received 6th September 2024,
Accepted 15th January 2025

DOI: 10.1039/d4nr03662j

rsc.li/nanoscale

Poly(phenylacetylene)s (PPAs) bearing *para*-substituted anilide pendant groups are sensitive to the presence of oxidizing metal ions such as Cu^{2+}, Hg^{2+}, Fe^{3+}, Au^{3+} or Ce^{4+} due to a redox reaction between the anilide-PPA and the metal ion. Using a library of six different PPAs containing diverse chiral pendant groups connected to the PPA backbone through the N (anilide) or C (benzamide) atoms of an amide group used as a linker, it was found that anilide-PPAs are sensitive to oxidizing metal ions. In these polymers, and through a redox reaction, a radical species is delocalized along the polyene backbone, resulting in a color change of the solution from yellow to blue. UV-Vis, ECD, IR, EPR, XPS and computational studies were carried out to demonstrate the electron transfer from PPA to the oxidizing metal once the metal coordinates with the anilide of the polymer.

Dynamic helical polymers, such as poly(phenylacetylene)s (PPAs),[1–14] are macromolecular helical switches whose *P* or *M* helical sense and elongation can be modulated by the presence of external stimuli such as pH, temperature, chiral additives, and anions among others.[15–18] Other interesting external stimuli to play with the dynamic response helical polymers are metal ions.[19] Heavy metal contamination of water and soil is a major problem found worldwide, which is associated with severe health problems. Thus, over the last few years several analytical methods have been used to detect and remove these metals.[20–22] Helical polymers such as PPAs have been designed to interact with these chemical agents to form helical polymer-metal complexes (HPMCs), where coordination of the metal ions with the pendant groups can occur in different ways: coordination and chelation. As a result, various conformations in the pendant can be stabilized either by a single metal under various conditions or by different metals, giving rise in one case or the other to the selective adoption of a *P* or *M* helical structure with different degrees of stretching. Moreover, it is also possible to play with the translocation of the metal in the pendant group by tuning the oxidation state of the metal, which can also lead to helical structural changes (sense and elongation). HMPCs have been used not only to detect metals or tune the helical structures of PPAs but also to create nanospheres and PPA@metal nanoparticle (MNP) nanocomposites with dynamic macroscopic chiralities.[23–26] The selective *P* or *M* screw sense induction of PPAs by different metal ions has been used to create a three-state switchable chiral stationary phase, where by using a single chiral column (stationary phase) and different metal ion salts in the mobile phase it is possible to change the retention time of different racemates depending on the helical sense adopted by the PPA.[27] Moreover, PPAs have been also employed as chiral catalysts in asymmetric synthesis.[28,29]

In this work we want to explore the interactions of PPAs with oxidizing metal ions such as Cu^{2+}, Hg^{2+}, Fe^{3+}, Au^{3+} and Ce^{4+} and where the PPA should act as a reducing agent. These metals, *e.g.* Hg^{2+}, Cu^{2+} or Fe^{+3}, are associated with health problems such as impaired mental and neurological functions (Hg^{2+}),[30,31] Alzheimer's disease, gastrointestinal problems and osteoporosis (Cu^{2+}),[32,33] and respiratorial, nervous system or reproductive or digestive system problems (Fe^{3+}).[34,35]

From the literature, it is known that PPAs can produce radical species along the polymer backbone[36–39] when subjected to high pressures[39] or mechanochemical grinding.[40] Hence, we hypothesized that PPAs containing a suitable pendant group can interact with oxidizing metals to form a PPA radical cation that can be further delocalized along the polyene backbone. To perform these studies, a library of six different chiral PPAs (Fig. 1) was chosen due to their stimuli-responsive properties towards metal ions. Thus, while in the case of poly-(**4–6**) the *P*/*M* helical sense can be controlled by the presence/absence of metal ions, regardless of the valence of the metal ion, poly-**1** can adopt a *P* or *M* helix in the presence of metal ions with different valences (Fig. 2).[15,18] Poly-

Centro Singular de Investigación en Química Biolóxica e Materiais Moleculares and Departamento de Química Orgánica Universidade de Santiago de Compostela Santiago de Compostela, Spain. E-mail: felix.freire@usc.es

†Electronic supplementary information (ESI) available. See DOI: https://doi.org/10.1039/d4nr03662j

‡These authors contributed equally to this work.

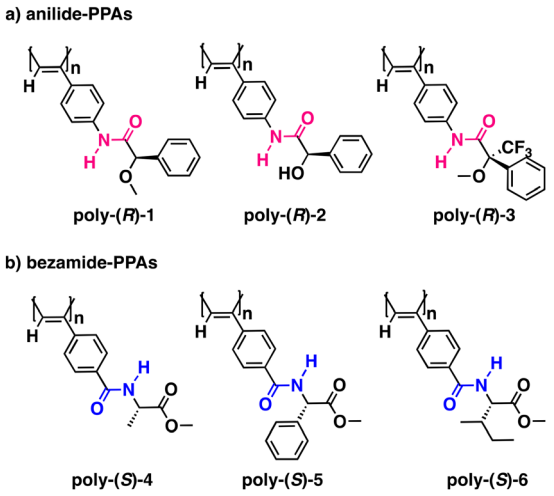

Fig. 1 Chemical structures of (a) anilide- and (b) benzamide-PPAs.

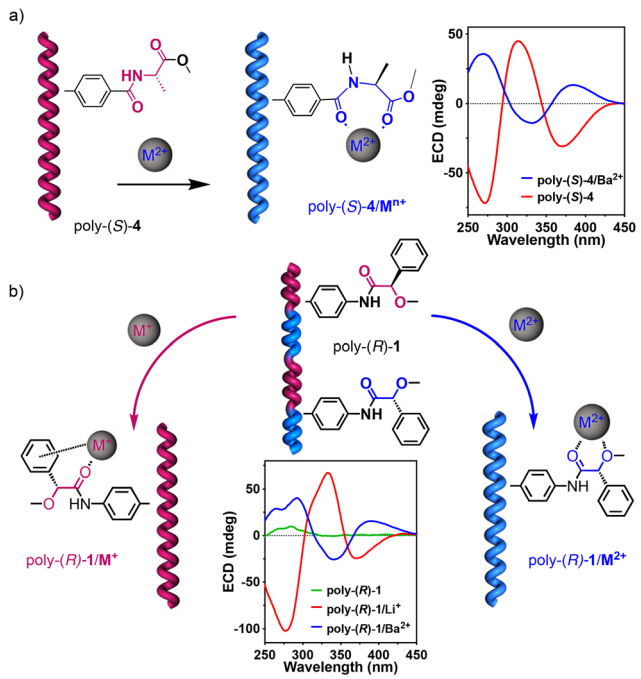

Fig. 2 Stimuli-responsive helical behavior of (a) poly-(*S*)-**4** and poly-(*R*)-**1** in the presence of 0.1 equivalents of metal ions.

(**1**–**6**) polymers were prepared according to the literature. Vials containing solutions of poly-(**1**–**6**) in THF (concn = 0.1 mg mL^{-1}) were then prepared and 1 equiv. of $Fe(ClO_4)_3$ (10 mg mL^{-1}, THF) was added to each. Interestingly, vials containing anilide-PPAs, poly-(**1**–**3**), immediately showed a color change from yellow to deep blue. The other vials containing benzamide-PPAs [poly-(**4**–**6**)] did not show any color change after the addition of $Fe(ClO_4)_3$.

This color change was ascribed to the presence of a delocalized radical ion along the polyene chain. IR studies revealed, as expected, the coordination of Fe^{3+} ions with carbonyl groups ($\Delta\bar{\nu} = 10\ cm^{-1}$) (Fig. S7†).

The existence of the radical ion was inferred from EPR studies (THF), which show a broad signal with a *g* value of 2.0039 confirming the presence of organic free radicals (Fig. 3b). UV-Vis studies (THF) show the disappearance of the polyene band at *ca.* 400 nm and the generation of a new band at *ca.* 600 nm (Fig. 3c). This band corresponds to a delocalization of the radical along the polyene backbone which is accompanied by an irreversible *cis*-to-*trans* isomerization of the double bonds (Fig. 3a). As a result, the helical structure of anilide-PPAs is lost, which can be monitored by ECD in those chiral anilide-PPAs that show a screw sense excess, such as poly-(**2**–**3**), where the ECD signal disappears once Fe^{3+} is added (Fig. 3e and S13†).

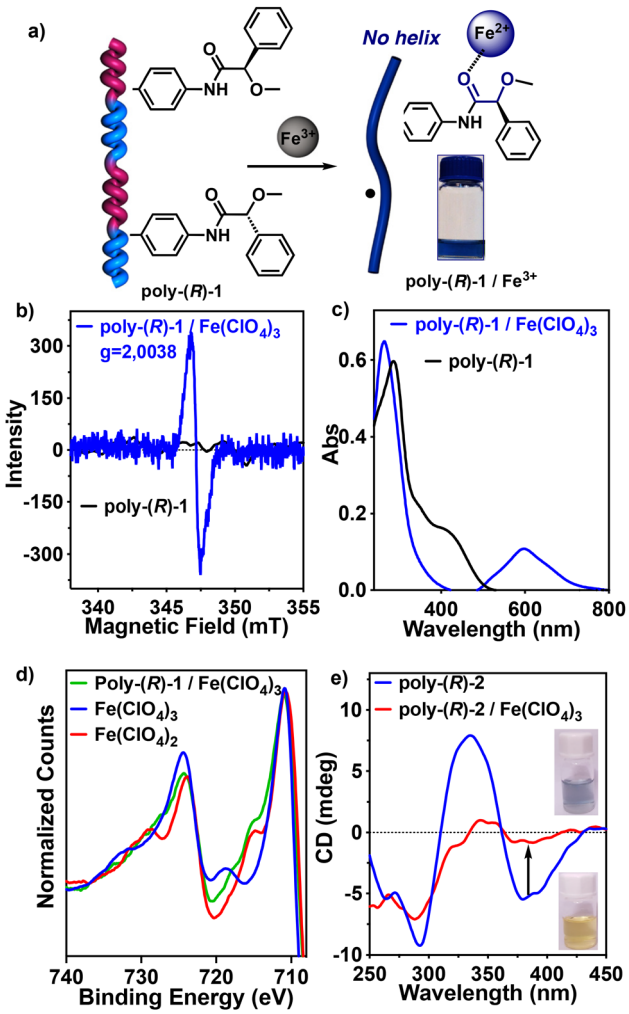

Fig. 3 (a) Conceptual illustration showing the formation of a poly-(*R*)-**1**/Fe^{3+} complex and the delocalized radical along the backbone. (b) EPR studies of poly-(*R*)-**1** and poly-(*R*)-**1**/Fe^{3+} complex in a 1.00/0.01 (mol/mol) ratio (THF). (c) UV-Vis studies of poly-(*R*)-**1** and a poly-(*R*)-**1**/Fe^{3+} complex in a 1.00/0.05 (mol/mol) ratio [poly-(*R*)-**1**] = 0.1 mg mL^{-1}, THF. (d) XPS studies of $Fe(ClO_4)_2$, $Fe(ClO_4)_3$ and poly-(*R*)-**1**/Fe^{3+} complex indicating the presence of Fe^{2+} after the oxidation of Fe^{3+}. (e) CD experiments of poly-(*R*)-**2** and a poly-(*R*)-**2**/Fe^{3+} complex in a 1.00/0.50 (mol/mol) ratio.

Fe^{3+} is a strong oxidizing agent,[41,42] so, to confirm that a redox process is taking place between the anilide-polymers and the Fe^{3+} ions, X-ray photoelectron spectroscopy (XPS) studies were carried out to determine the oxidation state of the iron before and after the addition of an anilide-polymer. As a control, XPS studies were carried out on commercially available iron salts—$Fe(ClO_4)_3$ and $Fe(ClO_4)_2$—to obtain the XPS spectra of the oxidation states of Fe^{3+} and Fe^{2+}. Next, XPS studies were performed for the poly-(*R*)-**1**/Fe^{3+} complex. Interestingly, the spectrum matches that obtained for $Fe(ClO_4)_2$, indicating that Fe^{3+} is reduced to Fe^{2+} after complexation with the anilide-polymer (Fig. 3d) generating a radical cation in the polymer.

To demonstrate that the oxidizing metal ion (Fe^{3+}) and an anilide-PPA are necessary to trigger the redox process, the same experiment was performed for the M-(*R*)-**1** monomer. Thus, $Fe(ClO_4)_3$ was added to a THF solution of M-(*R*)-**1**, which does not produce any color change in the solution. Moreover, EPR studies confirm the absence of radical species in a THF solution of the M-(*R*)-**1**/Fe^{3+} complex (Fig. S19†). This study indicates that the redox reaction is not triggered by the anilide group itself, and it needs to be linked to a phenylacetylene backbone.

Next, to determine the role of the anilide-connector in the redox reaction between an anilide-PPA and Fe^{3+} ions, we proceeded towards methylating the amide group of poly-(*R*)-**1** obtaining poly-(*R*)-**7** (see the ESI† for details of the synthesis). The addition of 1 equiv. of $Fe(ClO_4)_3$ (10 mg mL^{-1}, THF) to a THF solution of poly-(*R*)-**7** (concn = 0.1 mg mL^{-1}) did not produce any color change in the polymer solution (Fig. 4a and c). IR studies indicate coordination of the metal ion to the carbonyl group due to a shift in the carbonyl band ($\Delta\tilde{\nu}_{(CO)} = 50\ cm^{-1}$) (Fig. 4d). Moreover, EPR studies for a THF solution of poly-(*R*)-**7**/Fe^{3+} did not show the presence of radical species in the solution (Fig. S18†) and UV-Vis studies did not show any effect on the polyene band at *ca.* 400 nm (Fig. 4b), which confirms the absence of a radical cation delocalized along the polyene backbone. These studies indicate that the redox process between an anilide PPA and the Fe^{3+} ions is triggered by a synergistic effect between the anilide group used as a pendant and the PPA backbone, and not by just one of these two components of the helical polymer.

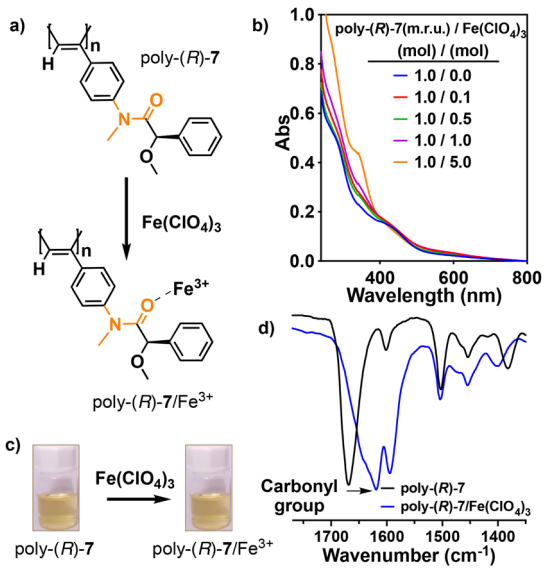

Fig. 4 (a) Illustration showing the formation of a poly-(*R*)-**7**/Fe^{3+} complex. (b) UV-Vis studies of poly-(*R*)-**1** and a poly-(*R*)-**1**/Fe^{3+} complex [poly-(*R*)-**1**] = 0.1 mg mL^{-1}, THF. (c) Images of vials containing solutions of poly-(*R*)-**7** and a poly-(*R*)-**7**/Fe^{3+} complex in THF. (d) FT-IR spectra of poly-(*R*)-**7** and poly-(*R*)-**7**/$Fe(ClO_4)_3$.

Thereafter, to determine the role of the anilide/Fe^{3+} interaction in the redox reaction, we added the oxidant metal ion salt to solutions of poly-(*R*)-**1** in non-coordinating and coordinating solvents such as $CHCl_3$ and DCM or DMF and DMSO, respectively. From these studies it was observed that a color change from yellow to blue also takes place in the presence of non-coordinating solvents, while in coordinating solvents no color changes are observed due to the lack of interaction between the polymer and the metal ion (Fig. S6†). These studies confirm that coordination between the anilide and the oxidizing metal ion is necessary to activate the redox reaction. The use of other oxidizing molecules such as hydrogen peroxide does not produce any effect on the polymer, indicating the need for interaction between the oxidizing agent and the polymer to trigger the redox reaction (see the ESI†).

Afterwards, theoretical calculations were carried out to corroborate the *cis* to *trans* isomerization of the double bonds and the consequent delocalization of the cation radical in the polyene backbone. Thus, DFT calculations—using the uB3LYP functional and the 6-31G* basis set with charge 1+ and doublet multiplicity—were performed first using the Gaussian16 software on an $n = 8$ oligomer of poly-(*R*)-**1** with a *trans*-configuration of double bonds. Analogous calculations were carried out for an $n = 9$ oligomer of poly-(*R*)-**1** with a *cis*-configuration of double bonds (see the ESI†). Spin density and SOMO show that the cation radical delocalizes from the pendant to the polyene backbone in the *trans* isomers (Fig. 5a and S26, S27†). On the other hand, the spin density of the *cis*-isomer isolates the radical at one edge of the oligomer, without delocalization (Fig. S25†).[43–46] TD-DFT calculations were then run to simulate the UV-Vis spectra using the u/rCAM-B3LYP functional and the 6-31G* basis set from the optimized geometries in DFT (see the ESI†). As expected, the experimental absorption band of the radical cation at 600 nm coincides with the calculated one (Fig. 5c). Furthermore, EPR calculations performed in Orca software using the UKS B3LYP functional and the EPR-II basis set predicted the same *g* values and EPR spectra as the experimental ones (Fig. 5b and S26†).

Finally, to extend the stimuli-responsive behavior of anilide-PPAs to other oxidizing metal ions, metal salts containing oxidizing metals such as Cu^{2+}, Hg^{2+}, Au^{3+} and Ce^{4+} were added to THF solutions of poly-(*R*)-**1** (0.1 mg mL^{-1}). In all cases, a color change from yellow to blue was observed with the appearance of a new band in the UV-Vis spectra at *ca.* 600 nm, confirming the presence of a delocalized radical cation along the polyene

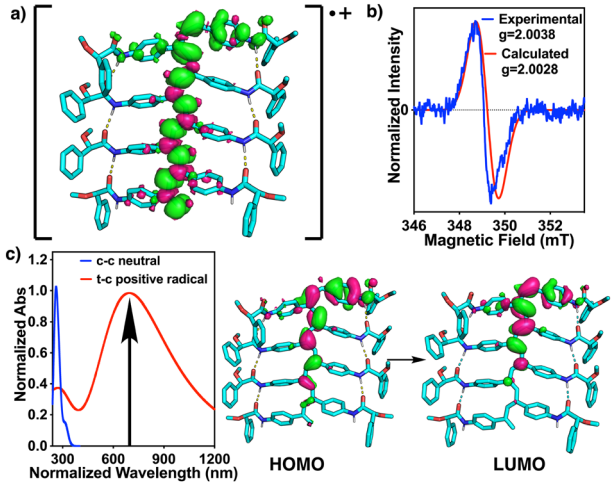

Fig. 5 (a) Spin density of a radical cation oligomer with a *trans-cisoidal* structure. (b) Comparison between the experimental EPR of poly-(*R*)-**1**/Fe^{3+} and that calculated for the *trans-cisoidal* oligomer. (c) Simulated UV-Vis spectra of the neutral *cis-cisoidal* oligomer and the radical cation *trans-cisoidal* oligomer. Transition attributed to the band at *ca.* 700 nm in the radical cation *trans-cisoidal* oligomer.

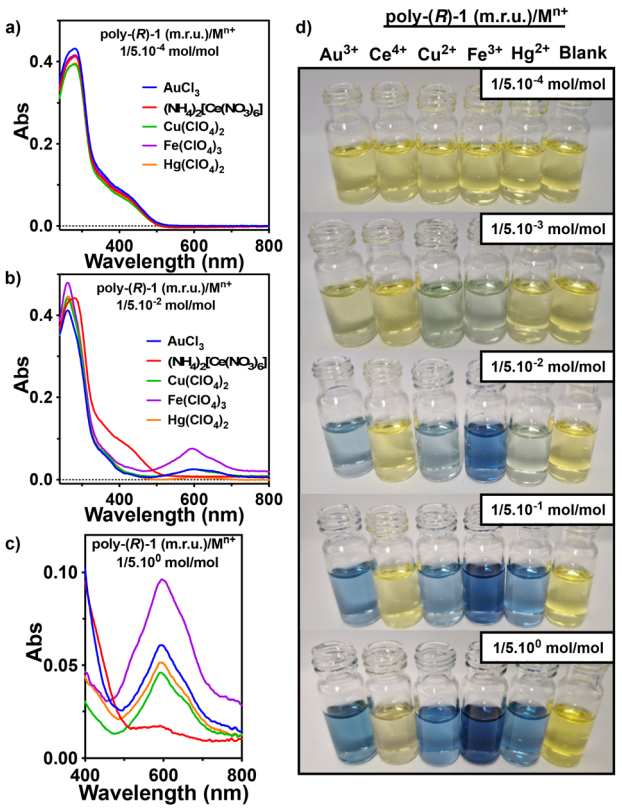

Fig. 6 (a–c) UV-Vis of poly-(*R*)-**1** (0.1 mg mL^{-1}, THF) in the presence of different equiv. of $Cu(ClO_4)_2$, $Fe(ClO_4)_3$, $Hg(ClO_4)_2$, and $AuCl_3$ (10.0 mg mL^{-1} and 1.0 mg mL^{-1}, THF) or $(NH_4)_2[Ce(NO_3)_6]$ (10.0 mg mL^{-1} and 1.0 mg mL^{-1}, MeOH). (d) Image of vials containing different THF solutions of several poly-(*R*)-**1**/M^{2+} complexes at different mol/mol ratios.

backbone. Again, these results show that anilide-PPAs are sensitive to the presence of oxidizing metal ions (Fig. 6a–d and S10, S11†). Titration experiments of a THF solution of poly-(*R*)-**1** with different equivalents of metal salts containing Cu^{2+}, Hg^{2+}, Au^{3+} or Fe^{3+} were performed to obtain the limit of detection (LOD) of the different poly-(*R*)-**1**/M^{n+} complexes (Fig. S11†). From these studies, the following LOD values were found when the concentration of poly-(*R*)-**1** was 0.1 mg mL^{-1} THF: 2.37 ppm for poly-(*R*)-**1**/Cu^{2+}; 8.41 ppm for poly-(*R*)-**1**/Hg^{2+}; 1.65 ppm for poly-(*R*)-**1**/Au^{3+} and 1.32 ppm for poly-(*R*)-**1**/Fe^{3+} (see Fig. S28 and Tables S1, S2†).

In conclusion, we have shown that anilide-PPAs are sensitive to the presence of oxidizing metal ions such as Cu^{2+}, Hg^{2+}, Fe^{3+}, Au^{3+} and Ce^{4+}. The coordination of the metal ions with the carbonyl group of the anilide is accompanied by an oxidation of the PPA, which produces a radical cation that delocalizes along the polyene backbone ($PPA^{\bullet+}$), while the metal ion is reduced. Delocalization of the polyene radical generates an irreversible *cis* to *trans* isomerization of the double bonds that results in the loss of the helical structure.

Furthermore, this delocalization of the radical cation along the polyene gives rise to an observable and effective colorimetric response from a yellow to deep blue solution. Therefore, dynamic helical polymers, such as anilide-PPAs, can be considered multi-stimuli-responsive materials that can respond differently to various families of metal ions. For instance, poly-(*R*)-**1** adopts an *M* helix in the presence of monovalent metal ions, a *P* helix with divalent metal ions, and has a colorimetric response when interacting with oxidizing metal ions. This work should therefore be inspiring for scientists working with stimuli-responsive materials, where a single design can sense diverse stimuli in different ways.

Data availability

The data supporting this article have been included as part of the ESI.†

Conflicts of interest

There are no conflicts to declare.

Acknowledgements

Financial support from AEI (PID2022-136848NB-I00), Xunta de Galicia (ED431C 2022/21, Centro Singular de Investigación de Galicia acreditación 2023–2027, ED431G 2023/03), and the European Regional Development Fund (ERDF) are gratefully acknowledged. M. N.-M. and M. F.-M. thank MICINN for an FPI contract (BES-2016-078107 and PID2019-109733GB-I00). We also thank Centro de Supercomputación de Galicia (CESGA) for computational resources.

References

1 S. Wang, J. Chen, X. Feng, G. Shi, J. Zhang and X. Wan, *Macromolecules*, 2017, **50**, 4610.
2 E. Yashima, K. Maeda, H. Iida, V. Furusho and K. Nagai, *Chem. Rev.*, 2009, **109**, 6102.
3 E. Schwartz, M. Koepf, H. Kitto, R. J. M. Nolte and A. E. Rowan, *Polym. Chem.*, 2011, **2**, 33.
4 J. Liu, J. W. Y. Lam and B. Z. Tang, *Chem. Rev.*, 2009, **109**, 5799.
5 V. Percec and Q. Xiao, *Isr. J. Chem.*, 2021, **61**, 530.
6 E. Yashima, K. Maeda and V. Furusho, *Acc. Chem. Res.*, 2008, **41**, 1166.
7 F. Freire, E. Quiñoá and R. Riguera, *Chem. Rev.*, 2016, **116**, 1242.
8 M. Lago-Silva, M. Fernández-Míguez, R. Rodríguez, E. Quiñoá and F. Freire, *Chem. Soc. Rev.*, 2024, **53**, 793.
9 N. Liu, R.-T. Gao and Z.-Q. Wu, *Acc. Chem. Res.*, 2023, **56**, 2954.
10 L. Zhou, C.-L. Li, R.-T. Gao, S.-M. Kang, L. Xu, X.-H. Xu, N. Liu and Z.-Q. Wu, *Macromolecules*, 2021, **54**, 679.
11 Z.-Q. Wu, X. Song, Y.-X. Li, L. Zhou, Y.-Y. Zhu, Z. Chen and N. Liu, *Nat. Commun.*, 2023, **14**, 566.
12 K. Maeda, M. Nozaki, K. Hashimoto, K. Shimomura, D. Hirose, T. Nishimura, G. Watanabe and E. Yashima, *J. Am. Chem. Soc.*, 2020, **142**, 7668.
13 K. Echizen, T. Taniguchi, T. Nishimura and K. Maeda, *Angew. Chem., Int. Ed.*, 2022, **61**, e202202676.
14 T. Kai, K. Nakamura, K. Mizumoto, K. Oki and E. Yashima, *Angew. Chem., Int. Ed.*, 2023, **62**, e202301127.
15 S. Arias, M. Núñez-Martinez, E. Quiñoá, R. Riguera and F. Freire, *Polym. Chem.*, 2017, **8**, 3740.
16 E. Suárez-Picado, E. Quiñoá, R. Riguera and F. Freire, *Angew. Chem., Int. Ed.*, 2020, **59**, 4537.
17 F. Rey-Tarrío, R. Rodríguez, E. Quiñoá and F. Freire, *Nat. Commun.*, 2023, **17**, 1742.
18 F. Freire, J. M. Seco, E. Quiñoá and R. Riguera, *Angew. Chem., Int. Ed.*, 2011, **50**, 11692.
19 C. Zhao, S. Meng, H. Chan, X. Wang, H. Li and M. C. W. Chan, *Angew. Chem., Int. Ed.*, 2022, **61**, e202115712.
20 F. S. A. Khan, N. M. Mubarak, Y. H. Tan, M. Khalid, R. R. Karri, R. Walvekar, E. C. Abdullah, S. Nizamuddin and S. A. Mazari, *J. Hazard. Mater.*, 2021, **413**, 100559.
21 X. Zhou, *Int. J. Electrochem. Sci.*, 2024, **19**, 100561.
22 M. Li, Q. Shi, N. Song, Y. Xiao, L. Wang, Z. Chen and T. D. James, *Chem. Soc. Rev.*, 2023, **52**, 5827.
23 M. Nuñez-Martínez, S. Arias, E. Quiñoá, R. Riguera and F. Freire, *Chem. Mater.*, 2021, **33**, 4805.
24 M. Nuñez-Martínez, E. Quiñoá and F. Freire, *Nanoscale*, 2022, **14**, 13066.
25 M. Núñez-Martínez, E. Quiñoá and F. Freire, *Chem. Mater.*, 2023, **35**, 4865.
26 M. Fernández-Míguez, M. Núñez-Martínez, E. Quiñoá and F. Freire, *ACS Nano*, 2024, **18**(42), 28822.
27 D. Hirose, A. Isobe, E. Quiñoá, F. Freire and K. Maeda, *J. Am. Chem. Soc.*, 2019, **141**, 8592.
28 H. Iida, Z. Tang and E. Yashima, *J. Polym. Sci., Part A: Polym. Chem.*, 2013, **51**, 2869.
29 L. M. S. Takata, H. Iida, K. Shimomura, K. Hayashi, A. A. dos Santos and E. Yashima, *Macromol. Rapid Commun.*, 2015, **36**, 2047.
30 K. Vikrant and K.-H. Kim, *Chem. Eng. J.*, 2019, **358**, 264.
31 R. Li, H. Wu, J. Ding, W. Fu, L. Gan and Y. Li, *Sci. Rep.*, 2017, **7**, 46545.
32 A. B. Tabrizi, *J. Hazard. Mater.*, 2007, **139**, 260.
33 M. R. Awual, M. Ismael, T. Yaita, S. A. El-Safty, H. Shiwaku, Y. Okamoto and S. Suzuki, *Chem. Eng. J.*, 2013, **222**, 67.
34 T. J. Huat, J. Camats-Perna, E. A. Newcombe, N. Valmas, M. Kitazawa and R. Medeiros, *J. Mol. Biol.*, 2019, **431**, 1843.
35 M. Halon-Golabek, A. Borkowska, A. Herman-Antosiewicz and J. Antosiewicz, *Front. Neurosci.*, 2019, **13**, 165.
36 E. Ohta, H. Sato, S. Ando, A. Kosaka, T. Fukushima, D. Hashizume, M. Yamasaki, K. Hasegawa, A. Muraoka, H. Ushiyama, K. Yamashita and T. Aida, *Nat. Chem.*, 2010, **3**, 68.
37 H. Iida, T. Mizoguchi, S.-D. Oh and E. Yashima, *Polym. Chem.*, 2010, **1**, 841.
38 E. Gomar-Nadal, J. Veciana, C. Rovira and D. B. Amabilino, *Adv. Mater.*, 2005, **17**, 2095.
39 K. Huang, Y. Mawatari, A. Miyasaka, Y. Sadahiro, M. Tabata and Y. Kashiwaya, *Polymer*, 2007, **48**, 6366.
40 A. Miyasaka, Y. Mawatari, T. Sone and M. Tabata, *Polym. Degrad. Stab.*, 2007, **92**, 253.
41 J. Pan, J. Li, R. Huang, X. Zhang, H. Shen, Y. Shion and X. Zhu, *Tetrahedron*, 2015, **71**, 5341.
42 X. Shi, X. Ren, Z. Ren, J. Li, Y. Wang, S. Yang, J. Gu, Q. Gao and G. Huang, *Eur. J. Org. Chem.*, 2014, 5083.
43 M. Peaks, C. Tait, P. Neuhaus, G. Fischer, M. Hoffmann, R. Haver, A. Cnossen, J. Harmer, C. Timmel and H. Anderson, *J. Am. Chem. Soc.*, 2017, **139**, 10461.
44 G. Moise, L. Tejerina, M. Rickhaus, H. Anderson and C. Timmel, *J. Phys. Chem. Lett.*, 2019, **10**, 5708.
45 Y. Yang, O. Blacque, S. Sato and M. Juríček, *Angew. Chem., Int. Ed.*, 2011, **60**, 13529.
46 C. R. Jacob and M. Reiher, *Int. J. Quantum Chem.*, 2012, **112**, 3661.